

STATIC TEST INDUCED LOADS VERIFICATION BEYOND ELASTIC LIMIT

V. Verderaine,* and F. Harrington*
 NASA Marshall Space Flight Center Alabama 35812

Abstract

NASA-TM-111443

roduction

Increasing demands for reliable and least-cost high-performance aerostructures are pressing design analyses, materials, and manufacturing processes to new and narrowly experienced performance and verification technologies. This study assessed the adequacy of current experimental verification of the traditional binding ultimate safety factor¹ which covers rare events in which no statistical design data exist. Because large high-performance structures are inherently very flexible, boundary rotations and deflections under externally applied loads approaching fracture may distort their transmission and unknowingly accept submarginal structures or prematurely fracturing reliable ones. A technique was developed, using measured strains from back-to-back surface mounted gauges, to analyze, define, and monitor induced moments and plane forces through progressive material changes from total-elastic to total-inelastic zones within the structural element cross section. Deviations from specified test loads are identified by the consecutively changing ratios of moment-to-axial load.

Nomenclature

N	= normal load, kips
M	= moment, kip-inches
C	= cross sectional limits, inches
H	= element thickness, inches
w	= element width, inches
E	= elastic modulus, ksi
n	= strain hardening exponent
K	= strength coefficient, ksi
σ	= normal stress, ksi
ϵ	= normal strain

Subscripts

t_y	= tensile yield
t_u	= tensile ultimate
c_y	= compression yield
N	= normal
M	= bending
1	= minimum measured strain
2	= maximum measured strain
k	= zone number

* Aerospace Engineers, Structures and Dynamics Laboratory

Copyright: ©1995 by the American Institute of Aeronautics and Astronautics, Inc. No copyright is asserted in the United States under Title 17, U.S. Code. The U.S. Government has royalty-free license to exercise all rights under the copyright claimed herein for government purposes. All other rights are reserved by the copyright owner.

Increasing demands for more reliable and affordable access to space are promoting leaner and more innovative structural designs that invoke more reliance on experimental verification of their behavior and safety. This compelling shift raises concerns on how well verification tests are implemented. Assemblies of large, high-performance aerostructures are inherently very flexible, and structural boundary rotations and deflections at externally applied loads approaching rupture may improperly transmit the binding verification loads and unknowingly reject a perfectly adequate design or accept a submarginal one.

To sample this phenomenon, the slope and deflection were calculated at the free-end boundary load on a hypothetical cantilevered beam, Fig. 1. Deflections and slopes are shown for the yield and ultimate strain limits calculated at the fixed end. The tangent of the free boundary slope θ is a measure of the consecutively applied load decomposing from bending to bending-axial load ratio. Though the vertical scale is exaggerated, the slopes and displacements at the free end are proportional.

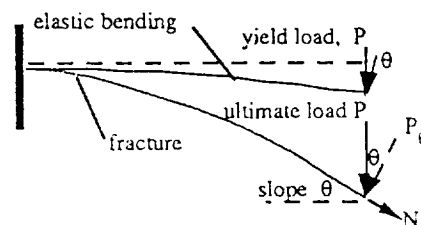


Fig. 1. Boundary load deformation

The ultimate load to fracture was calculated to be twice the yield load, and the resulting ultimate strain at the fixed end was an order-of-magnitude larger than the yield. At ultimate loading, the predicted deflection was an 18 degree slope resulting in over 30 percent bending-to-axial load ratio deviation. The adversity of this ratio to the verification criteria is dependent on how it feeds into and intensifies critically stressed regions and how it may change the failure mode.

Though many codes and texts are available for predicting inelastic strain responses from imposed inplane and bending loads, literature is mute on determining test combined loads from measured inelastic strains. A technique was developed to analyze elastic-inelastic strains measured from back-to-back surface mounted gauges to determine and verify transmitted test loads with specified applied loads.

II. Elastic-inelastic materials model

Modeling elastic-inelastic behavior could be very difficult² unless idealized into the simplest mathematical

expressions within the physical phenomena of the material and its application, such as the two parameter power expression,³

$$\sigma = K \epsilon^n, \quad (1)$$

where "n" is the strain-hardening exponent. In the linear elastic region, $\sigma \leq F_y$, the exponent is defined as $n = 1.0$, and for $\sigma > F_y$, the strain-hardening exponent is calculated from uniaxial stress-strain data

$$n = \frac{\log (F_u / F_y)}{\log (\epsilon_u / \epsilon_y)}. \quad (2)$$

The strength coefficient "K" is evaluated at the yield stress, which is the elastic-inelastic interface,

$$K = \frac{F_y}{\epsilon_y^n} = E^n F_y^{(1-n)}. \quad (3)$$

These properties are directly applicable to normal stresses and strains without interpretation through theory.

III. Structural Modeling

A rectangular cross section element illustrated in Fig 2 represents most structural components and regions as in beams, plates, and shells. Bending and inplane normal loadings are the most commonly measured components on this type of element using back-to-back strain gauges. They often may be sufficient to sample and verify the load transmission of more complex systems, including transverse shears.

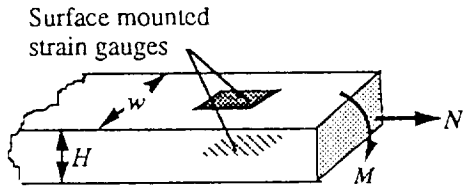


Fig. 2. Back-to-back instrumented element

The induced normal stress in Fig. 2,

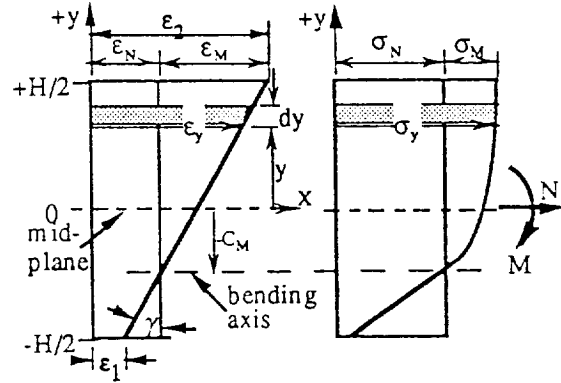
$$\sigma_N = \frac{N}{w H}, \quad (4)$$

and strain,

$$\epsilon_N = \left[\frac{N}{K w H} \right]^{\frac{1}{n}}, \quad (5)$$

are uniformly distributed over the element cross section throughout the elastic and inelastic range. Because cross section planes are known to remain plane after elastic and inelastic bending, the inelastic bending strain also varies linearly along the thickness. However, the stress varies nonlinearly with Eq. (1) and the bending neutral axis is not expected to coincide with the cross section centroid. Since

bending and axial strains are linear, they may be algebraically added as shown in figure 3(a). These combined strains are measured back-to-back at the element surfaces as ϵ_2 and ϵ_1 , where ϵ_2 is assumed to be greater than ϵ_1 . Fig. 3(b) illustrates the nonlinear bending stress distribution derived from the strain distribution using Eq. (1) and the shift of the bending axis to balance the moment.



3(a) combined strain 3(b) combined stress

Fig. 3. Strain and stress distributions along the element cross section

When $\epsilon_2 < \epsilon_{iy}$, the combined strain distributions over the cross section are all in one elastic zone, and when $\epsilon_1 > \epsilon_{iy}$, the distributions are all in one inelastic zone. The objective is to define the elastic-inelastic zone boundaries for all other measured strain combinations and to calculate their contributions to the total normal and bending loads.

The net strain from any midplane y-distance along the element thickness in figure 3(a) is defined by the proportionality

$$\epsilon_y = \gamma (0.5 H + y) + \epsilon_1, \quad (6)$$

and its location is

$$y = \frac{1}{\gamma} (\epsilon_y - \epsilon_1) - 0.5 H. \quad (7)$$

The bending strain slope is

$$\gamma = \frac{\epsilon_2 - \epsilon_1}{H}. \quad (8)$$

The incremental normal load along the cross section thickness is the product of the induced stress and area,

$$dN = w \sigma_y dy = w K (\epsilon_y)^n dy.$$

Substituting Eq. (6) for the strain and integrating, all zone normal loads may be calculated from

$$N_k = \frac{wK\gamma^n}{n+1} \left[\frac{H}{2} + \frac{\epsilon_1}{\gamma} + y \right]^{n+1} \Big|_{C_b}^{C_a} \quad (9)$$

where C_a and C_b are the integration limits of a zone. A zone is bound along the y -axis by the surface measured strains, ϵ_1 and ϵ_2 , or by the material limit changes noted by ϵ_{ty} and ϵ_{cy} . Substituting the appropriate pair of boundary strains into Eq. (7),

$$C_{a,b} = \frac{1}{\gamma} (\epsilon_{a,b} - \epsilon_1) - \frac{H}{2} \quad (10)$$

provides the upper and lower integration limits of each zone. The yield strain may be tension or compression, where $\epsilon_{cy} = -\epsilon_{ty}$ is assumed for a symmetrical material. The normal load across the thickness is the sum of all the zone normal loads

$$N = \sum N_k \quad (11)$$

Bending strain along the thickness is given by $\epsilon_{My} = \epsilon_y - \epsilon_N$, and the neutral bending axis is defined by a zero bending strain ($\epsilon_{My} = 0$), from which $\epsilon_y = \epsilon_N$. Substituting into Eq. (7), the neutral bending axis is

$$C_M = \frac{1}{\gamma} (\epsilon_N - \epsilon_1) - 0.5 H \quad (12)$$

where the normal strain, ϵ_N , across the thickness is determined by substituting Eq. (11) into Eq. (5). Using Eq. (12), the incremental moment about the neutral axis is

$$dM = w\sigma_y(y - C_M) dy = wK(\epsilon_y)^n(y - C_M) dy \quad (13)$$

Substituting Eq.s (6) and (12) into Eq. (13) and integrating, a zone moment about the neutral axis is calculated from

$$M_k = wK\gamma \left[\frac{H}{2} + \frac{\epsilon_1}{\gamma} + y \right]^{n+1} \times \left\{ \frac{\frac{H}{2} + \frac{\epsilon_1}{\gamma} + y}{n+2} - \frac{\frac{H}{2} + \frac{\epsilon_1}{\gamma} + C_M}{n+1} \right\} \Big|_{C_b}^{C_a} \quad (14)$$

The moment about the cross section is the sum of all the zone moments,

$$M = \sum M_k \quad (15)$$

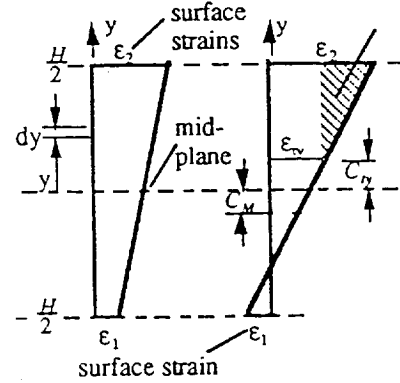
A unit width, $w = 1$, is assumed for plates and shells from which normal loads and bending moments are defined by kips per inch and kip-inch per inch units, respectively. Using the strain distribution expression of Eq. (6), the stress distribution along each zone is given by

$$\sigma_y = K [ABS(\epsilon_y)]^n SGN(\epsilon_y) \quad (16)$$

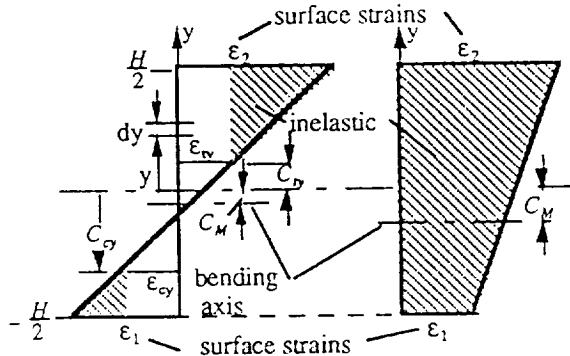
Expressions in absolute form allow raising strains to odd powers. $SGN(\)$ is the signum function, which re-establishes the sign of the expression. If the function equals -1, the strain is negative.

IV. Normal Load and Moment Solutions

As the induced normal and bending loads in figure 2 increase, the strain distribution over the element cross section progresses from totally elastic to totally inelastic in four possible profiles. Given the values of the two measured strains, ϵ_1 and ϵ_2 , the related profile is directly selected, and the zones and integration limits are decided as shown in figure 4.



(I) $\epsilon_{cy} < \epsilon_1 < \epsilon_2 < \epsilon_{ty}$ (II) $\epsilon_{cy} < \epsilon_1 < \epsilon_{ty} < \epsilon_2$



(III) $\epsilon_1 < \epsilon_{cy} < \epsilon_{ty} < \epsilon_2$ (IV) $\epsilon_{ty} < \epsilon_1 < \epsilon_2$

Fig. 4. Strain profiles over element cross section

The induced combined normal and bending moment loads in each strain profile are resolved through a straightforward analytical routine summarized as follows:

- Using azone boundaries strains from selected Fig. 4 profile, the integration limits $C_{a,b}$ for each zone are defined from Eq. (10), and are substituted into Eq. (9) to solve for the normal load $N_{I,k}$ of each zone in the profile,

- The sum of normal loads from all zones, Eq. (11), is substituted into Eq. (5) to obtain the profile normal strain.

- The bending neutral axis C_M is located using the total normal strain from Eq. (5) in Eq. (12)

- Equation (14) determines the bending moment $M_{I,k}$ in each zone about the neutral bending axis, which are summed in Eq. (15) to provide the desired profile moment.

- Strain distribution ϵ_y and stress distribution σ_y are plotted over the thickness using Eqs. (6) and (16), respectively.

This direct, though laborious, routine was reduced to a simple computer code requiring no detailed knowledge of its derivation.

V. Normal-bending loads program

Profile (III), having the most zones, was solved and programmed as summarized above. Other profiles, having fewer zones, were adapted by resetting limits according to their zone boundary values and positions in the strain diagrams and applying them to their appropriate zones.

NORMAL/BENDING LOADS FROM STRAIN DATA
'NMLFSD, Microsoft Quick Basic

' MATERIAL PROPERTIES

```
INPUT "ELASTIC MODULUS E=";ELM
INPUT "YIELD STRESS Fty=";FTY
INPUT "MAX STRESS Ftu=";FTU
INPUT "STRAIN @ MAX STRESS Etw=";ETU
```

```
ETY=FTY/ELM
PRINT "TENSION YIELD STRAIN";ETY
ECY=-ETY
SHE=LOG(FTU/FTY)/LOG(ETU/ETY)
PRINT "STRAIN HARDENING EXPO. n=";SHE
K=FTY/(ETY^SHE)
PRINT "STRENGTH COEF K=";K
K0=K
SHE0=SHE
ECY0=ECY
ETY0=ETY
```

'TEST DATA

```
INPUT "ELEMENT THICKNESS H=";H
INPUT "ELEMENT WIDTH w=";W
```

```
10 INPUT "TEST MAX STRAIN E2=";E2
INPUT "TEST MIN STRAIN E1=";E1
IF E2<E1 THEN
PRINT "MAX STRAIN < MIN STRAIN"
GOTO 10
END IF
IF E2=E1 THEN E1=0.975
SLOP=(E2-E1)/H
```

PRO=3

```
USING PROFILE (III) (E1<ECY<ETY<E2)
IF ECY<E1 AND E1<ETY AND ETY<E2 THEN
ECY=E1:PRO=2
ELSEIF ETY<E1 AND E1<E2 THEN
ECY=E1:ETY=E1:PRO=4
ELSEIF E2<ETY AND ECY<E1 THEN
K=ELM:SHE=1:ECY=E1:ETY=E2:PRO=1
END IF
```

```
NIII1=W*K*(E2^(SHE+1)-
ETY^(SHE+1))/(SLOP*(SHE+1))
NIII2=W*ELM*((ETY^2)-(ECY^2))/(2*SLOP)
NIII3=(ABS(ECY)^(SHE+1)-(ABS(E1)^(SHE+1))
NIII3=NIII3*W*K/(SLOP*(SHE+1))
NIIIT=NIII1+NIII2+NIII3
PRINT "TOTAL AXIAL LOAD N=";NIIIT
SNIII=NIIIT/W/H
PRINT "AXIAL LOAD STRESS SN=";SNIII
```

```
IF SNIII<FTY THEN
ENIII=SNIII/ELM
ELSE
ENIII=(SNIII/K)^(1/SHE)
END IF
PRINT "AXIAL LOAD STRAIN EN=";ENIII
EMMIII=E2-ENIII
PRINT "MAX BENDING STRAIN EM=";EMMIII
```

```
CMIII=(ENIII-E1)/SLOP-H/2
PRINT "BENDING NEUTRAL AXIS CM=";CMIII
```

```
MIII1=-((E2^(SHE+1))-(ETY^(SHE+1)))/(SHE+1)
MIII1=MIII1*((E1+E2)/2+CMIII*SLOP)
MIII1=MIII1+((E2^(SHE+2))-(ETY^(SHE+2)))/(SHE+2)
MIII1=MIII1*W*K/(SLOP^2)
MIII2=-((ETY^2)-(E1^2))*((E1+E2)/2+CMIII*SLOP)/2
MIII2=MIII2+((ETY^3)-(E1^3))/3
MIII2=MIII2*W*ELM/(SLOP^2)
MIII3=-((ABS(ECY)^(SHE+1))-
(ABS(E1)^(SHE+1)))/(SHE+1)
MIII3=MIII3*((E1+E2)/2+CMIII*SLOP)
MIII3=MIII3+((ABS(ECY)^(SHE+2))-
(ABS(E1)^(SHE+2)))/(SHE+2)
MIII3=MIII3*W*K/(SLOP^2)
MIIIT=MIII1+MIII2+MIII3
PRINT "BENDING MOMENT M=";MIIIT
```

```
RIII=MIIIT/NIIIT
PRINT "MOMENT/AXIAL LOAD RATIO R=";RIII
```

' LIMITS

```
CTY=(ETY-E1)/SLOP-H/2
CCY=(ECY-E1)/SLOP-H/2
ETYA=FTY/ELM
```

' STRESS & STRAIN DISTRIBUTIONS
OPEN "CLIP:" FOR OUTPUT AS #2

```
PRINT "PROFILE=";PRO
```

```

IF PRO=3 THEN
YS=-.5*H: YF=CCY: MY=9
M=MY-1
DY=(YF-YS)/M
EY3=0: SY3=0
y=YS
FOR I=1 TO M
EY3=(.5*H+y)*SLOP+E1
SY3=K*((ABS(EY3)^SHE))*SGN(EY3)
WRITE #2,y,EY3,ENIII,ETYA,SY3,SNIII,FTY
PRINT y,EY3,ENIII,ETYA,SY3,SNIII,FTY
y=YS+(I+1)*DY
NEXT I
END IF

IF PRO=1 OR PRO=2 OR PRO=3 THEN
YS=CCY: YF=CTY: MY=9
IF E2<ETY THEN YF=.5*H
M=MY-1
DY=(YF-YS)/M
EY2=0: SY2=0
y=YS
FOR I=1 TO M
EY2=(.5*H+y)*SLOP+E1
SY2=ELM*EY2
WRITE #2,y,EY2,ENIII,ETYA,SY2,SNIII,FTY
PRINT y,EY2,ENIII,ETYA,SY2,SNIII,FTY
y=YS+(I+1)*DY
NEXT I
END IF

IF PRO=2 OR PRO=3 OR PRO=4 THEN
YS=CTY: YF=.5*H: MY=11
M=MY-1
DY=(YF-YS)/M
EP1=0: SP1=0
y=YS
FOR I=1 TO M
EP1=(.5*H+y)*SLOP+E1
SP1=K*((ABS(EP1)^SHE))*SGN(EP1)
WRITE #2,y,EP1,ENIII,ETYA,SP1,SNIII,FTY
PRINT y,EP1,ENIII,ETYA,SP1,SNIII,FTY
y=YS+(I+1)*DY
NEXT I
END IF

CLOSE #2
REM STOP
CLS
ETY=ETY0
ECY=ECY0
K=K0
SHE=SHE0
GOTO 10

```

A sample printout of the program giving cross section characteristics derived from back-to-back strain gauge data is

```

ELASTIC MODULUS E=? 10500
YIELD STRESS Fty =? 38
MAX STRESS Ftu =? 58
STRAIN @ MAX STRESS Eyu =? .06
TENSION YIELD STRAIN 3.619048E - 03
STRAIN HARDENING EXPO. n = .1505829
STRENGTH COEF K= 88.59669
ELEMENT THICKNESS H=? 1.4
ELEMENT WIDTH w=? .74
TEST MAX STRAIN E2=? .02
TEST MIN STRAIN E1=? -.01
TOTAL AXIAL LOAD N= 16.21604
AXIAL LOAD STRESS SN= 15.65255
AXIAL LOAD STRAIN EN= 1.490719E-03
MAX BENDING STRAIN EM= 1.850928E-02
BENDING NEUTRAL AXIS CM= -.1637665
BENDING MOMENT M= 17.29161
MOMENT / AXIAL LOAD RATIO R= 1.066328

```

VI. Conclusions

Experimental verification consists of two coherent, deterministic static test parts. Structural response within the elastic limit is verified with specified external loads representing maximum predicted operational environments. The ultimate factor of safety covers rare events, and its traditional and historical usage exerts the greatest influence on design and acceptance criteria.

However, the order-of-magnitude larger strains, and therefore displacements, imposed by the ultimate factor of safety may distort the applied load transmission. The documented technique was developed to identify and assess verification load transfer discrepancy through back-to-back surface mounted strain gauge data, which is applicable throughout the elastic and inelastic range of the structural material.

It is concerning that verification test results often report surface strain measurements to conform very well with predicted math models up to the yield point, but then unexpectedly deviate during the inelastic loading to premature fracture. Reasons offered are usually indefinite. Perhaps this suggested technique may extend the basis for a more definite test evaluation.

References

1. Anon; "Structural Factor of Safety and Test Verification", NASA White paper, Oct. 9, 1992.
2. Phillips, A.; "Introduction to Plasticity", The Ronald Press Company, 1956.
3. Dieter, G. ; "Mechanical Metallurgy", 3rd edition, McGraw-Hill, Inc., NY., 1986.